

# The top-pair forward-backward asymmetry beyond NLO

Valentin Ahrens,<sup>1</sup> Andrea Ferroglia,<sup>2</sup> Matthias Neubert,<sup>1</sup> Ben D. Pecjak,<sup>1</sup> and Li Lin Yang<sup>3</sup>

<sup>1</sup>*Institut für Physik (THEP), Johannes Gutenberg-Universität, D-55099 Mainz, Germany*

<sup>2</sup>*New York City College of Technology, 300 Jay Street, Brooklyn, NY 11201, USA*

<sup>3</sup>*Institute for Theoretical Physics, University of Zürich, CH-8057 Zürich, Switzerland*

(Dated: February 5, 2022)

We make use of recent results in effective theory and higher-order perturbative calculations to improve the theoretical predictions of the QCD contribution to the top-quark pair production forward-backward asymmetry at the Tevatron. In particular, we supplement the fixed-order NLO calculation with higher-order corrections from soft gluon resummation at NNLL accuracy performed in two different kinematic schemes, which allows us to make improved predictions for the asymmetry in the  $p\bar{p}$  and  $t\bar{t}$  rest frames as a function of the rapidity and invariant mass of the  $t\bar{t}$  pair. Furthermore, we provide binned results which can be compared with the recent measurements of the forward-backward asymmetry in events with a large pair invariant mass or rapidity difference. Finally, we calculate at NLO+NNLL order the top-quark charge asymmetry at the LHC as a function of a lower rapidity cut-off for the top and antitop quarks.

## I. INTRODUCTION

The forward-backward (FB) asymmetry in top-quark pair production in proton-antiproton collisions is an observable which originates from the difference in the production rates for top quarks in the forward and backward hemispheres [1, 2]. The total FB asymmetry was measured by the CDF and D0 collaborations at the Tevatron [3–5]. The measurement can be carried out in the laboratory frame ( $p\bar{p}$  frame) as well as in the center-of-mass frame of the top-quark pair ( $t\bar{t}$  frame). The asymmetries in the two frames are defined as

$$A_{\text{FB}}^i = \frac{N(y_t^i > 0) - N(y_t^i < 0)}{N(y_t^i > 0) + N(y_t^i < 0)}, \quad (1)$$

where  $N$  is the number of events,  $i = p\bar{p} (t\bar{t})$  indicates the laboratory frame ( $t\bar{t}$  frame), and  $y_t^i$  is the top-quark rapidity in frame  $i$ . The measurements obtained by the CDF collaboration using  $5.3 \text{ fb}^{-1}$  of data are [5]

$$\begin{aligned} A_{\text{FB}}^{p\bar{p}} &= (15.0 \pm 5.5)\% \quad (p\bar{p} \text{ frame}), \\ A_{\text{FB}}^{t\bar{t}} &= (15.8 \pm 7.5)\% \quad (t\bar{t} \text{ frame}). \end{aligned} \quad (2)$$

The quoted uncertainties are derived from a combination of statistical and systematic errors.

The production of top-quark pairs at hadron colliders is dominated by QCD. At the Tevatron, the charge conjugation invariance of the strong interaction implies that the difference in the production of top quarks in the forward and backward hemispheres is equivalent to the difference in the production of top and antitop quarks in the forward hemisphere. Therefore, in QCD the FB asymmetry is equivalent to the charge asymmetry. QCD predicts a non-vanishing contribution to the FB asymmetry starting at order  $\alpha_s^3$  in the squared amplitude. A contribution to the asymmetry arises if, in the interference of one-loop and tree-level diagrams, the top-quark fermionic line and the light-quark fermionic line are connected by three gluons [2]. The same is true in the case of the interference of two tree-level diagrams with three particles in the final state. The dominant effect is from the quark-antiquark annihilation channel, while a further, numerically small contribution to the asymmetry at order  $\alpha_s^3$  originates from the flavor excitation channel  $gq \rightarrow t\bar{t}X$ , where  $X$  indicates additional partons in the final state. The gluon fusion channel does not contribute to the FB asymmetry at any order in perturbation theory, due to the fact that the gluon distribution is the same for protons and antiprotons.

The total FB asymmetry predicted by QCD at the first non-vanishing order (which, for reasons discussed later in this paper, we will indicate as next-to-leading order (NLO)) is lower than the one measured at the Tevatron. Two recent evaluations using the formulas in [2] report the following values [6, 7], obtained using MSTW2008 NLO parton distribution functions (PDFs) [8],

$$\begin{aligned} A_{\text{FB}}^{p\bar{p}, \text{NLO}} &= (4.8_{-0.4}^{+0.5})\% \quad (p\bar{p} \text{ frame}), \\ A_{\text{FB}}^{t\bar{t}, \text{NLO}} &= (7.4_{-0.6}^{+0.7})\% \quad (t\bar{t} \text{ frame}). \end{aligned} \quad (3)$$

The central values quoted in (3) refer to the choice  $\mu_f = m_t$ , where  $\mu_f$  is the factorization scale and  $m_t$  the top-quark mass, which is set to  $m_t = 173.1 \text{ GeV}$ . The errors originate from the scale variation in the range  $m_t/2 \leq \mu_f \leq 2m_t$ .

These choices will also be adopted in the rest of the paper. Electroweak corrections enhance the prediction for the asymmetry by less than 10% of the central value [2, 9], and to separate uncertainties coming from electroweak calculations we do not include these corrections in our numerical results. As one can see, the discrepancy between the theory prediction and the experimental measurement in the  $p\bar{p}$  frame is less than two standard deviations ( $2\sigma$ ), while in the  $t\bar{t}$  frame the two values agree within  $\sim 1\sigma$ , although the central value of the experimental measurement is a bit higher.

In [5], the CDF collaboration measured the FB asymmetry in the  $t\bar{t}$  frame as a function of the top-pair invariant mass  $M_{t\bar{t}}$ . After grouping the events in two bins corresponding to  $M_{t\bar{t}} \leq 450$  GeV and  $M_{t\bar{t}} \geq 450$  GeV, they found the asymmetry in the latter bin to be

$$A_{\text{FB}}^{t\bar{t}}(M_{t\bar{t}} \geq 450 \text{ GeV}) = (47.5 \pm 11.4)\%, \quad (4)$$

which is more than  $3\sigma$  higher than the stated theoretical NLO prediction in [5] of  $(8.8 \pm 1.3)\%$  obtained using the MCFM program [10]. A measurement of the FB asymmetry in two bins of the rapidity difference  $y_t - y_{\bar{t}}$  was also performed and again in that case the higher bin shows a tension with the NLO QCD prediction, although with larger experimental errors. Many attempts to explain these results in terms of new physics scenarios have been made, see e.g. [11–21]. The task is complicated by the fact that the new physics contributions should not spoil the good agreement between theory and measurements for the total pair-production cross section and the differential distribution in the pair invariant mass.

Recently, we have calculated the top-pair invariant-mass distribution and the top-quark rapidity and transverse-momentum distributions in renormalization-group (RG) improved perturbation theory, which incorporates the resummation of logarithmic corrections that become numerically large in the limit of soft-gluon emission [6, 7]. These calculations were carried out at next-to-next-to-leading-logarithmic (NNLL) accuracy. The resummed distributions were then matched to the NLO results to obtain predictions which have NLO+NNLL accuracy. Alternatively, the resummed results at NNLL order can be employed to generate approximate next-to-next-to leading (NNLO) predictions [6, 7]. We note that working at approximate NNLO accuracy does not alter in a fundamental way any of the results obtained within the NLO+NNLL framework. On the other hand, we believe that in certain kinematic regions, for instance at large pair invariant mass, resummation is important. For these reasons, and for the sake of simplicity, in the following we focus on NLO+NNLL calculations. By integrating the differential distributions it is then straightforward to calculate the top-quark FB asymmetry both in the laboratory frame and in the  $t\bar{t}$  frame. Starting from the double differential cross section in the pair invariant mass and scattering angle, we can also compute the  $M_{t\bar{t}}$  and rapidity-dependent asymmetries, which can be compared to experimental measurements. The main goal of this letter is to present the result of these calculations of the total and differential FB asymmetries in a systematic way.

At the Large Hadron Collider (LHC), the symmetry of the  $pp$  initial state dictates that the rapidity distributions of the top and antitop quarks are symmetric and that the FB asymmetry vanishes. However, it was observed in [2] that at the LHC top quarks are preferably produced at larger rapidities than antitop quarks in the laboratory frame. Like the FB asymmetry at the Tevatron, this rapidity-dependent charge asymmetry is generated at order  $\alpha_s^3$  in the squared amplitude, mainly through the asymmetric part of the quark-antiquark annihilation channel. Therefore, potential new physics contributions would effect these two quantities in a correlated way, and the higher collider energy at the LHC gives it better access to distortions at higher rapidities. As a final application of our formalism, we evaluate at NLO+NNLL order the partially integrated charge asymmetry at the LHC, giving results as a function of a lower cut-off on the top and antitop rapidities in the laboratory frame.

## II. FB ASYMMETRY IN THE LABORATORY FRAME

### A. Total asymmetry

The FB asymmetry in the laboratory frame can be calculated starting from the top-pair production cross section differential with respect to the top-quark transverse momentum  $p_T$  and rapidity  $y_t$ . To do so, it is convenient to first define a total and differential asymmetric cross section via

$$\begin{aligned} \Delta\sigma_{\text{FB}}^{p\bar{p}} &\equiv \int_0^{y_t^+} dy_t \left[ \int_0^{p_T^{\text{max}}} dp_T \frac{d^2\sigma^{p\bar{p} \rightarrow tX_{\bar{t}}}}{dp_T dy_t} - \int_0^{p_T^{\text{max}}} dp_T \frac{d^2\sigma^{p\bar{p} \rightarrow tX_{\bar{t}}}}{dp_T d\bar{y}_t} \Big|_{\bar{y}_t = -y_t} \right] \\ &\equiv \int_0^{y_t^+} dy_t \left[ \left( \frac{d\sigma}{dy_t} \right)_F - \left( \frac{d\sigma}{dy_t} \right)_B \right] \equiv \int_0^{y_t^+} dy_t \frac{d\Delta\sigma_{\text{FB}}^{p\bar{p}}}{dy_t}. \end{aligned} \quad (5)$$

Here

$$y_t^+ = \frac{1}{2} \ln \frac{1 + \sqrt{1 - 4m_t^2/s}}{1 - \sqrt{1 - 4m_t^2/s}} \quad \text{and} \quad p_T^{\max} = \frac{\sqrt{s}}{2} \sqrt{\frac{1}{\cosh^2 y_t} - \frac{4m_t^2}{s}}, \quad (6)$$

where  $s$  is the square of the hadronic center-of-mass energy. To obtain the FB asymmetry in the laboratory frame one needs to calculate the ratio of the asymmetric cross section in (5) to the total cross section:

$$A_{\text{FB}}^{p\bar{p}} = \frac{\Delta\sigma_{\text{FB}}^{p\bar{p}}}{\sigma}. \quad (7)$$

In our phenomenological analysis we will consider two levels of perturbative precision for the asymmetric cross section and FB asymmetry. The first involves the differential cross section at NLO in fixed-order perturbation theory, the second the NLO calculation supplemented with soft-gluon resummation to NNLL order. In the laboratory frame, the resummed calculations are carried out using the 1PI<sub>SCE</sub>T scheme introduced in [7]. Such predictions resum a class of logarithms which become large in the limit where  $s_4 = (p_{\bar{t}} + k)^2 - m_t^2$  is small ( $p_{\bar{t}}$  indicates the momentum of the antitop quark, and  $k$  the total momentum of additional partons in the final state), in which case real gluon emission is soft although the top pair is not produced at rest. While the phase-space integrals in (5) are in general sensitive to regions where  $s_4$  is not small, the threshold region is dynamically enhanced due to the sharp fall-off of the PDFs away from small values of  $s_4$ . In fact, it was shown in [7] that the leading terms in the 1PI<sub>SCE</sub>T threshold limit reproduce essentially the entire NLO correction to the differential cross section in the quark channel, which implies that resumming the corrections which become large in this limit is an improvement on the fixed-order calculation. While in the fixed-order counting the asymmetric cross section first arises from the NLO calculation of the differential cross section, in the resummed counting it first appears at NLL order. The NLO+NNLL calculation is thus a refinement on the leading term, and will be considered our best prediction.

Before illustrating our results for the FB asymmetry, we need to clarify an important point concerning our convention for counting orders in the perturbative expansion. We calculate  $A_{\text{FB}}$  itself as a perturbative expansion in  $\alpha_s$ , using a fixed-order or logarithmic counting as appropriate. For example, the first non-vanishing contribution to the asymmetry in fixed-order perturbation theory is obtained by calculating the numerator in (7) to order  $\alpha_s^3$  and the denominator to order  $\alpha_s^2$ . The resulting asymmetry is of order  $\alpha_s$ , which we will refer to as NLO, with reference to the order at which the differential distributions in (5) are calculated relative to  $\alpha_s^2$ . Similarly, in RG-improved perturbation theory, the first non-vanishing contribution to  $A_{\text{FB}}$  is obtained by calculating both the numerator and the denominator at next-to-leading-logarithmic (NLL) order; the resulting asymmetry is then counted as NLL. This convention was already adopted in [6, 7]. There are two counting schemes in the literature (in fixed-order perturbation theory) which are different from ours. The first one also treats  $A_{\text{FB}}$  itself as a perturbative expansion, but counts the order  $\alpha_s$  contribution as LO, and so on, as in [1, 2]. The second one treats the numerator and the denominator as separate perturbative series and does not further expand the ratio, as adopted in the quoted MCFM results in [5]. We note that while the first scheme differs from ours only by name, the second scheme leads to different numerical results. As discussed in [6], the NLO+NNLL results are considerably more stable with respect to the choice of scheme than the NLO results.

	MSTW2008		CTEQ6.6		NNPDF2.1	
	$\Delta\sigma_{\text{FB}}^{p\bar{p}}$ [pb]	$A_{\text{FB}}^{p\bar{p}}$ [%]	$\Delta\sigma_{\text{FB}}^{p\bar{p}}$ [pb]	$A_{\text{FB}}^{p\bar{p}}$ [%]	$\Delta\sigma_{\text{FB}}^{p\bar{p}}$ [pb]	$A_{\text{FB}}^{p\bar{p}}$ [%]
NLO	$0.260^{+0.141+0.020}_{-0.084-0.014}$	$4.81^{+0.45+0.13}_{-0.39-0.13}$	$0.256^{+0.135}_{-0.082}$	$4.69^{+0.44}_{-0.38}$	$0.269^{+0.144}_{-0.086}$	$4.82^{+0.47}_{-0.38}$
NLO+NNLL	$0.312^{+0.027+0.023}_{-0.035-0.019}$	$4.88^{+0.20+0.17}_{-0.23-0.18}$	$0.319^{+0.026}_{-0.037}$	$4.79^{+0.17}_{-0.25}$	$0.335^{+0.029}_{-0.039}$	$4.93^{+0.22}_{-0.24}$

TABLE I: The asymmetric cross section and FB asymmetry in the  $p\bar{p}$  frame. The first error refers to perturbative uncertainties estimated through scale variations as explained in the text, and the second error in the MSTW2008 case is the PDF uncertainty.

Our results for the total FB asymmetry in the lab frame are shown in Table I. As explained above, to calculate each entry in the table the numerator and the denominator in (7) are evaluated at the order indicated in the leftmost column, and then the ratio itself is expanded in powers of  $\alpha_s$  up to the appropriate order. The central values are obtained by fixing the factorization scale at  $\mu_f = m_t$ , and the scale uncertainties are estimated by varying  $\mu_f$  between  $m_t/2$  and  $2m_t$ .<sup>1</sup> In the resummed calculations also the hard and soft scales are varied according to the procedure

<sup>1</sup> Although we use  $m_t = 173.1$  GeV throughout the analysis, the asymmetry is rather stable under the exact choice of  $m_t$ . For instance, at  $m_t = 160$  GeV the default value for the asymmetric cross section at NLO with MSTW2008 PDFs changes to  $\Delta\sigma_{\text{FB}}^{p\bar{p}} = 0.384$  pb, but the asymmetry itself changes only by a small amount to  $A_{\text{FB}}^{p\bar{p}} = 4.67\%$ .

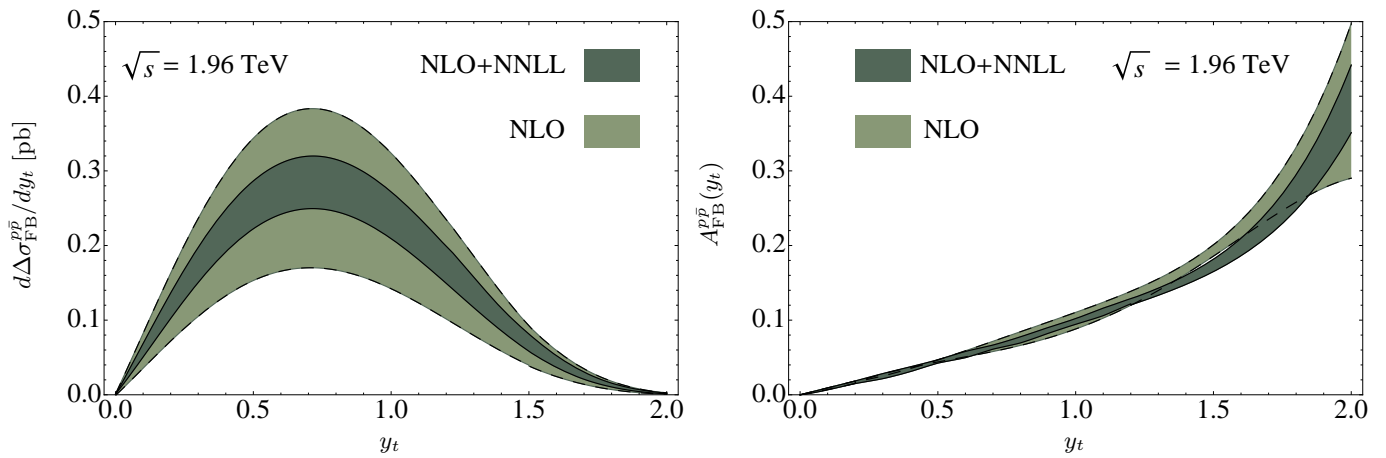


FIG. 1: Left: The asymmetric differential cross section  $d\Delta\sigma_{\text{FB}}^{pp}/dy_t$ . Right: The asymmetry  $A_{\text{FB}}^{pp}(y_t)$ . The bands show the uncertainties related to scale variation as explained in the text.

described in [7], and the effect of these variations is included in the scale uncertainty shown in the tables. In the first column of the table we use MSTW2008 PDFs and estimate the PDF uncertainties by iterating through the 90% confidence level (CL) sets. Here and throughout this work we use NLO PDFs for the NLO prediction, and switch to NNLO PDFs for the NLO+NNLL calculation. The PDF uncertainties for the asymmetry, expressed as a percentage of the central values, are about half as large as those for the asymmetric cross section. This is due to cancellations in the ratio. In addition to results with MSTW2008 PDFs, we also show those obtained using CTEQ6.6 [22] and NNPDF2.1 [23] PDFs. In those cases the PDFs are based on a NLO fit so that the same set is used in both the NLO and the NLO+NNLL calculations. We note that the results for the asymmetry obtained with the different PDF sets are well within the PDF uncertainties estimated through the MSTW2008 results.

Adding soft-gluon resummation at NNLL accuracy produces results for the asymmetric cross section which are numerically consistent with the NLO results for  $\mu_f = m_t$ , while the scale uncertainty is reduced by more than a factor of 2. The central value for the FB asymmetry does not change significantly with respect to the NLO predictions, and also in this case the scale uncertainties are reduced. We can therefore conclude that the discrepancy between theory and experiment cannot be explained with the effect of higher-order QCD corrections on the theory side, at least not those related to soft-gluon resummation.

The NLO+NNLL calculation represents the most accurate determination of the QCD contribution to the asymmetry that can be obtained at present. However, it is important to keep in mind the uncertainties related to yet higher-order corrections and how they could be reduced. Concerning soft gluon resummation, the most important improvement beyond NNLL accuracy would be the calculation of the hard and soft matching functions at NNLO order. This requires the soft plus virtual corrections at NNLO in QCD, and would fix the  $\delta$ -function contribution to the differential cross section at that order. In that case, the further improvement of matching the resummed results to fixed order would require power-suppressed effects related to hard gluon emission. The arguments based on the dynamical enhancement of the threshold region and the confirmation of this mechanism through the numerical results at NLO, imply that power corrections to the soft limit are small, so we expect the more important effect to be the calculation of the soft plus virtual corrections. We estimate uncertainties related to both types of corrections through the standard method of scale variations and the numerical results indicate that these higher-order effects are moderate. However, this statement can of course never be certain without the actual calculation of the higher-order pieces. Similar comments apply to all other quantities obtained in this work.

## B. Rapidity-dependent asymmetry

As experimental measurements become more precise, differential quantities such as the rapidity-dependent asymmetry can be compared with theoretical predictions. Using quantities defined in (5), we can write this differential

asymmetry as

$$A_{\text{FB}}^{p\bar{p}}(y_t) = \frac{\left(\frac{d\sigma}{dy_t}\right)_F - \left(\frac{d\sigma}{dy_t}\right)_B}{\left(\frac{d\sigma}{dy_t}\right)_F + \left(\frac{d\sigma}{dy_t}\right)_B} = \frac{\frac{d\Delta\sigma_{\text{FB}}^{p\bar{p}}}{dy_t}}{\left(\frac{d\sigma}{dy_t}\right)_F + \left(\frac{d\sigma}{dy_t}\right)_B}. \quad (8)$$

In Figure 1 we show results for the differential asymmetric cross section and the FB asymmetry as functions of the rapidity at NLO and NLO+NNLL order, using MSTW2008 PDFs. Here and below, the differential cross sections at NLO are obtained using a private NLO version of MadGraph [24]. The bands refer to uncertainties associated with scale variations. One observes that the NLO+NNLL band for the asymmetric differential cross section displayed in the left-hand panel is contained within the NLO band over the entire range of  $y_t$  values shown in the figure, and that the scale uncertainty of the NLO+NNLL asymmetric cross section is smaller than the scale uncertainty obtained in the NLO calculation. On the other hand, the differences between the error bands in the NLO and NLO+NNLL results for the FB asymmetry shown in the right-hand panel are much smaller due to cancellations in the ratio which make the NLO FB asymmetry considerably more stable than the corresponding asymmetric cross section. We will encounter this feature repeatedly in the  $t\bar{t}$ -frame calculations which follow. One observes that the form of the rapidity-dependent asymmetry, which is an increasing function with respect to  $y_t$ , is very stable under higher-order corrections.

### III. FB ASYMMETRY IN THE $t\bar{t}$ FRAME

#### A. Total asymmetry

Our studies of the FB asymmetry in the  $t\bar{t}$  rest frame will use as a fundamental quantity the top-pair production cross section differential with respect to the pair invariant mass and the top-quark scattering angle in that frame. We thus define an asymmetric cross section as

$$\begin{aligned} \Delta\sigma_{\text{FB}}^{t\bar{t}} &\equiv \int_{2m_t}^{\sqrt{s}} dM_{t\bar{t}} \left[ \int_0^1 d\cos\theta \frac{d^2\sigma^{p\bar{p}\rightarrow t\bar{t}X}}{dM_{t\bar{t}}d\cos\theta} - \int_{-1}^0 d\cos\theta \frac{d^2\sigma^{p\bar{p}\rightarrow t\bar{t}X}}{dM_{t\bar{t}}d\cos\theta} \right] \\ &\equiv \int_{2m_t}^{\sqrt{s}} dM_{t\bar{t}} \left[ \left(\frac{d\sigma}{dM_{t\bar{t}}}\right)_F - \left(\frac{d\sigma}{dM_{t\bar{t}}}\right)_B \right] \equiv \int_{2m_t}^{\sqrt{s}} dM_{t\bar{t}} \frac{d\Delta\sigma_{\text{FB}}^{t\bar{t}}}{dM_{t\bar{t}}}, \end{aligned} \quad (9)$$

and the total FB asymmetry in the  $t\bar{t}$  frame is then given by

$$A_{\text{FB}}^{t\bar{t}} = \frac{\Delta\sigma_{\text{FB}}^{t\bar{t}}}{\sigma}. \quad (10)$$

As in the previous section, we will study the FB asymmetry at both NLO and NLO+NNLL accuracy. In the  $t\bar{t}$  frame, the resummed calculations are carried out using the PIM<sub>SCET</sub> scheme introduced in [6]. The differential cross section calculated in that work includes the resummation of partonic threshold logarithms up to NNLL order directly in momentum space, and thus extends the previous results from [25], which included resummation to NLO+NLL accuracy in moment space. Such predictions resum a tower of logarithms which become large when the square of the pair invariant mass is close to the partonic center-of-mass energy:  $z = M_{t\bar{t}}^2/\hat{s} \rightarrow 1$ . In this limit real gluon emission is soft although, as in the case of 1PI kinematics, the top quarks are not necessarily produced at rest. While the soft limit  $z \rightarrow 1$  can be enforced kinematically by the restriction to large pair invariant mass, the phase-space integrals in (9) are in general sensitive to regions where this is not the case. However, the analysis of [6] showed that events near the partonic threshold provide the numerically dominant contributions to the differential cross section, even at low values of the invariant mass near the peak of the distribution, due to dynamical threshold enhancement from the PDFs [26], which indicates that resumming threshold logarithms is an improvement on the fixed-order calculation. The suppression of power corrections to the soft limit is also backed up by the negligible numerical difference between the calculation of the asymmetry in the  $t\bar{t}$  frame and the partonic center-of-mass frame. The results in these two frames coincide in the threshold limit  $z \rightarrow 1$ , and differ by only about 1% at NLO [6], due to very small corrections from hard gluon emission.<sup>2</sup>

<sup>2</sup> In [6], results at NLO+NNLL order for the total asymmetry were actually given in the partonic center-of-mass frame. In the present work, we have eliminated this small mismatch with the experimental measurements by working in the  $t\bar{t}$  frame.

	MSTW2008		CTEQ6.6		NNPDF2.1	
	$\Delta\sigma_{\text{FB}}^{t\bar{t}}$ [pb]	$A_{\text{FB}}^{t\bar{t}}$ [%]	$\Delta\sigma_{\text{FB}}^{t\bar{t}}$ [pb]	$A_{\text{FB}}^{t\bar{t}}$ [%]	$\Delta\sigma_{\text{FB}}^{t\bar{t}}$ [pb]	$A_{\text{FB}}^{t\bar{t}}$ [%]
NLO	$0.395^{+0.213+0.028}_{-0.128-0.021}$	$7.32^{+0.69+0.18}_{-0.59-0.19}$	$0.389^{+0.205}_{-0.123}$	$7.14^{+0.67}_{-0.54}$	$0.411^{+0.218}_{-0.131}$	$7.36^{+0.70}_{-0.58}$
NLO+NNLL	$0.448^{+0.080+0.030}_{-0.071-0.026}$	$7.24^{+1.04+0.20}_{-0.67-0.27}$	$0.461^{+0.083}_{-0.073}$	$7.16^{+1.05}_{-0.68}$	$0.486^{+0.088}_{-0.078}$	$7.39^{+1.08}_{-0.69}$

TABLE II: The asymmetric cross section and FB asymmetry in the  $t\bar{t}$  rest frame. The first error refers to perturbative uncertainties estimated through scale variations, and the second error in the MSTW2008 case is the PDF uncertainty.

Our numerical results for the total asymmetric cross section and FB asymmetry are summarized in Table II. As was the case in the laboratory frame, the scale uncertainties in the asymmetric cross section are roughly halved at NLO+NNLL order compared to NLO. The scale uncertainties in the FB asymmetry, on the other hand, actually increase slightly after adding the resummation, while the central values are nearly unchanged. We note however that the resummed results are more stable with respect to the scheme for expanding the ratio defining the FB asymmetry [6], and in that sense are more reliable than the NLO predictions. Moreover, the resummed results for both the asymmetric and total cross sections are more stable under scale variations than their fixed-order counterparts. One should therefore be cautious of the rather small scale uncertainties in the NLO calculation of the FB asymmetry, which result from large cancellations in the ratio not observed in the resummed result. We again show the PDF uncertainties using the MSTW2008 PDFs at 90% CL, and the central values and scale uncertainties from the CTEQ6.6 and NNPDF2.1 sets. All comments from the previous section concerning the reduction of PDF errors in the FB asymmetry compared to the asymmetric cross section, and the good agreement between the different PDF sets, are also true in this case.

### B. Invariant-mass dependent asymmetry

As mentioned in the introduction, the recent measurement of the asymmetry at high values of the pair invariant mass shows a large deviation from the value predicted by QCD at NLO. In order to examine the effects of soft-gluon resummation on this observable, we first extract from (9) the invariant-mass dependent asymmetry as

$$A_{\text{FB}}^{t\bar{t}}(M_{t\bar{t}}) = \frac{\left(\frac{d\sigma}{dM_{t\bar{t}}}\right)_F - \left(\frac{d\sigma}{dM_{t\bar{t}}}\right)_B}{\left(\frac{d\sigma}{dM_{t\bar{t}}}\right)_F + \left(\frac{d\sigma}{dM_{t\bar{t}}}\right)_B} = \frac{d\Delta\sigma_{\text{FB}}^{t\bar{t}}}{dM_{t\bar{t}}}. \quad (11)$$

Results for  $A_{\text{FB}}^{t\bar{t}}(M_{t\bar{t}})$  and  $d\Delta\sigma_{\text{FB}}^{t\bar{t}}/dM_{t\bar{t}}$  at NLO and NLO+NNLL order are shown in Figure 2, where the bands reflect uncertainties originating from scale variations. The figure shows that the asymmetry increases with the invariant mass and can reach nearly 40% at  $M_{t\bar{t}} = 1200$  GeV. These results are obtained with the default MSTW2008 PDFs and do not include PDF uncertainties. An analysis shows that the relative PDF error for  $d\Delta\sigma_{\text{FB}}^{t\bar{t}}/dM_{t\bar{t}}$  increases slightly with increasing  $M_{t\bar{t}}$ , from 7% (400 GeV) to 9% (1200 GeV). In contrast, the relative PDF error for  $A_{\text{FB}}^{t\bar{t}}(M_{t\bar{t}})$  is rather small and even decreases with  $M_{t\bar{t}}$ , from around 2% (400 GeV) to 1% (1200 GeV).

It is a well-known fact that electroweak corrections start to become more important for the differential cross section at high pair invariant mass, due to the presence of Sudakov logarithms. For instance, at  $M_{t\bar{t}} \sim 1$  TeV, the electroweak corrections to the differential distribution at the Tevatron are roughly at the -5% level [27, 28], even though for the total cross section they are negligible. On the other hand, the electroweak corrections to the asymmetric cross section given in [2] do not contain Sudakov logarithms, and an estimate shows that their distortion of the QCD contribution is roughly independent of the invariant mass. We therefore do not expect the electroweak corrections to significantly alter our results for the FB asymmetry even at high values of pair invariant mass.

We hope that better statistics can eventually lead to a detailed comparison of experimental results with the asymmetry curve in Figure 2. At present this is not possible, but the CDF collaboration has measured the invariant-mass dependent asymmetry by separating the events into a high invariant-mass bin ( $M_{t\bar{t}} \geq 450$  GeV) and a low invariant-mass bin ( $M_{t\bar{t}} \leq 450$  GeV) [5]. From Figure 2, one can see that this choice roughly divides the total asymmetric cross section equally between the two bins, although most of the asymmetric cross section in the high invariant-mass bin originates from the region close to 450 GeV. More precisely, the region 450 – 600 (700) GeV captures more than 75 (90)% of the total asymmetric cross section in the high invariant-mass bin. To compare with the CDF results, we

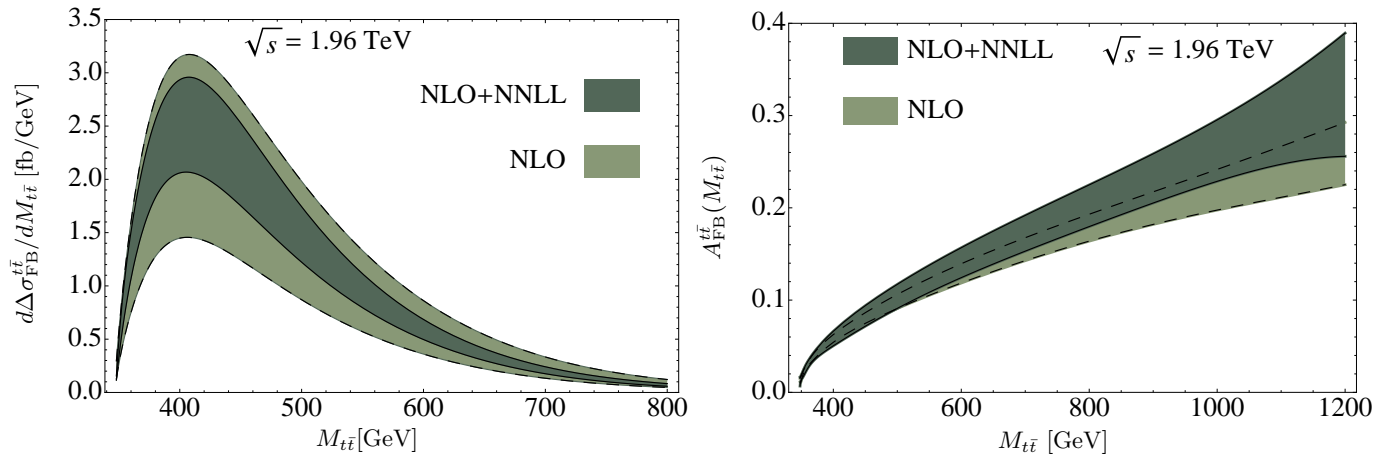


FIG. 2: Left: The asymmetric cross section  $d\Delta\sigma_{\text{FB}}^{t\bar{t}}/dM_{t\bar{t}}$  as a function of the invariant mass at NLO and NLO+NNLL order. Right: The asymmetry  $A_{\text{FB}}^{t\bar{t}}(M_{t\bar{t}})$ . The bands show the uncertainties related to scale variation as explained in the text.

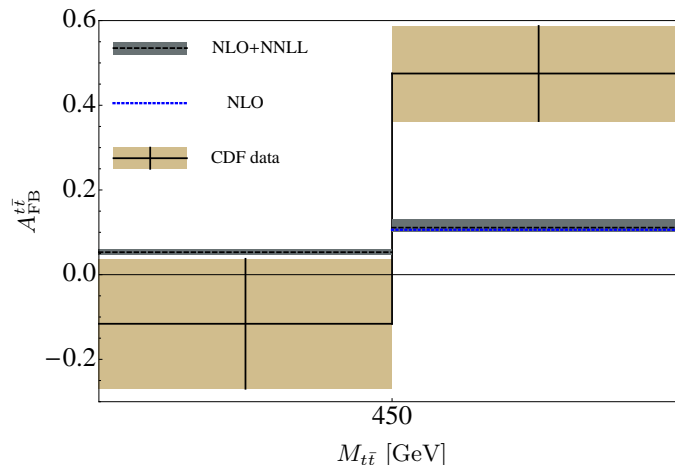


FIG. 3: The asymmetry in the high and low invariant-mass region as measured in [5], compared to our predictions at NLO+NNLL order. The bands in the NLO+NNLL results are related to uncertainties from scale variation, while the NLO result in the higher bin is evaluated at  $\mu_f = m_t$ .

evaluate the binned asymmetry

$$A_{\text{FB}}^{t\bar{t}}(m_1, m_2) = \frac{\int_{m_1}^{m_2} dM_{t\bar{t}} \left( d\Delta\sigma_{\text{FB}}^{t\bar{t}}/dM_{t\bar{t}} \right)}{\int_{m_1}^{m_2} dM_{t\bar{t}} (d\sigma/dM_{t\bar{t}})}, \quad (12)$$

for  $M_{t\bar{t}} \leq 450$  GeV and for  $M_{t\bar{t}} \geq 450$  GeV. Our findings are given in Table III, along with their visual representation in Figure 3, which shows the NLO+NNLL calculation with an error band from scale variations along with the default NLO number in the high invariant-mass bin. In both bins, the NLO+NNLL predictions for the asymmetric cross sections have considerably smaller scale uncertainties than the NLO ones, but the results for the FB asymmetries are essentially unchanged. As with all other results obtained in the  $t\bar{t}$  frame, the scale uncertainties in the FB asymmetries are larger in the NLO+NNLL calculation than at NLO. However, if we had not expanded the ratio, the predicted FB asymmetry in the high invariant-mass bin would be 9.0% at NLO and 10.6% at NLO+NNLL order<sup>3</sup>, showing the

<sup>3</sup> Using MSTW2008 PDFs as an example.

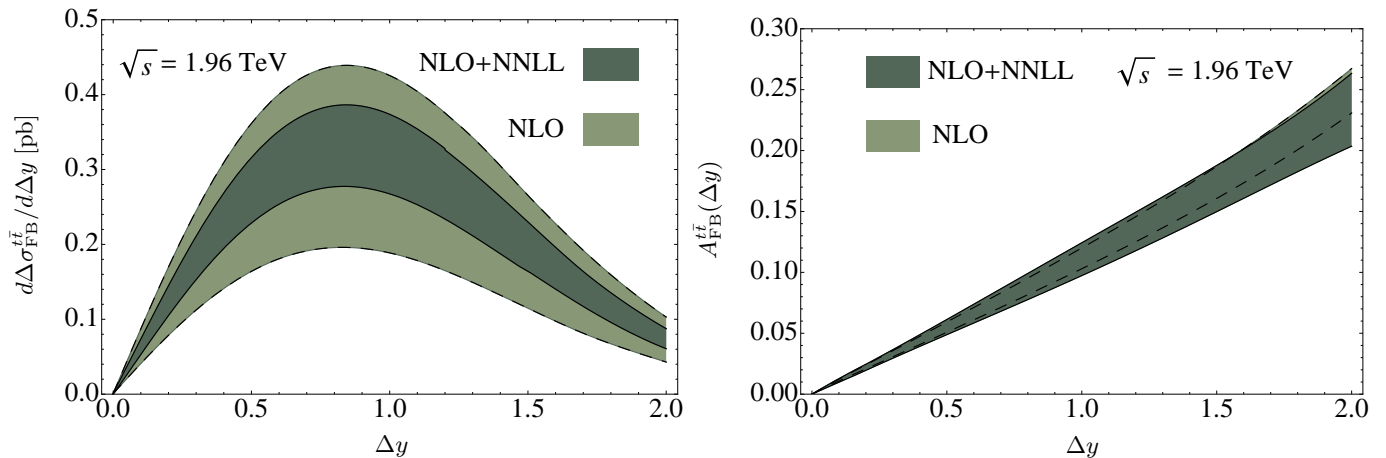


FIG. 4: Left: The asymmetric differential cross section  $d\Delta\sigma_{\text{FB}}^{t\bar{t}}/d\Delta y$ . Right: The asymmetry  $A_{\text{FB}}^{t\bar{t}}(\Delta y)$ . The bands show the errors related to scale variation as explained in the text.

stability of the resummed results under this change of systematics.

	$M_{t\bar{t}} \leq 450 \text{ GeV}$						$M_{t\bar{t}} > 450 \text{ GeV}$											
	$\Delta\sigma_{\text{FB}}^{t\bar{t}} [\text{pb}]$			$A_{\text{FB}}^{t\bar{t}} [\%]$			$\Delta\sigma_{\text{FB}}^{t\bar{t}} [\text{pb}]$			$A_{\text{FB}}^{t\bar{t}} [\%]$								
CDF							$-11.6^{+15.3}_{-15.3}$						$47.5^{+11.2}_{-11.2}$					
	MSTW	CTEQ	NNPDF	MSTW	CTEQ	NNPDF	MSTW	CTEQ	NNPDF	MSTW	CTEQ	NNPDF	MSTW	CTEQ	NNPDF			
NLO	$0.17^{+0.10}_{-0.05}$	$0.18^{+0.09}_{-0.05}$	$0.19^{+0.09}_{-0.06}$	$5.2^{+0.6}_{-0.2}$	$5.3^{+0.4}_{-0.4}$	$5.4^{+0.3}_{-0.4}$	$0.22^{+0.13}_{-0.07}$	$0.22^{+0.12}_{-0.07}$	$0.23^{+0.12}_{-0.07}$	$10.8^{+1.0}_{-0.8}$	$10.4^{+1.0}_{-0.6}$	$10.9^{+0.7}_{-0.6}$						
NLO+NNLL	$0.21^{+0.04}_{-0.03}$	$0.22^{+0.04}_{-0.04}$	$0.23^{+0.04}_{-0.04}$	$5.2^{+0.9}_{-0.6}$	$5.2^{+0.8}_{-0.6}$	$5.4^{+0.7}_{-0.6}$	$0.24^{+0.04}_{-0.04}$	$0.25^{+0.05}_{-0.04}$	$0.26^{+0.04}_{-0.04}$	$11.1^{+1.7}_{-0.9}$	$10.8^{+1.7}_{-0.9}$	$11.4^{+1.3}_{-1.0}$						

TABLE III: Comparison of the low- and high-mass asymmetry  $A_{\text{FB}}^{t\bar{t}}$  with CDF data [5], along with results for the asymmetric cross section. The errors in the QCD predictions refer to perturbative uncertainties related to scale variation.

We now turn to a discussion of the PDF uncertainties in the binned results, in this case deviating slightly from our usual procedure. The reason is that to compute the PDF uncertainties for the binned asymmetry at NLO+NNLL order, we need to run the Monte Carlo program MadGraph at NLO for each of the PDFs in the error set, which is rather time consuming. As a compromise, we have estimated the PDF uncertainties using only the pieces of the NLO calculation which are leading in the threshold limit  $M_{t\bar{t}}^2/\hat{s} \rightarrow 1$ , as obtained in [6]. Since these leading pieces alone account for the bulk of the NLO FB asymmetry, the relative PDF uncertainties obtained from these terms should provide a good approximation to those in the full NLO and NLO+NNLL results. For the MSTW2008 set, we find a relative PDF uncertainty of about 7% for the asymmetric cross section and about 2% for the FB asymmetry at 90% CL, in both the low and high invariant-mass bins.

Our calculations show that neither higher-order corrections from soft-gluon resummation nor the inclusion of a systematic uncertainty coming from PDF usage reduces in any significant way the current discrepancy between theory and experiment for the FB asymmetry in the high invariant-mass bin, which remains above the  $3\sigma$  level when using our NLO+NNLL calculations.

### C. Rapidity-dependent asymmetry

A further observable of interest is the rapidity dependence of the FB asymmetry in the  $t\bar{t}$  frame. In practice, experiments measure the asymmetry as a function of the pair rapidity difference  $\Delta y = y_t - y_{\bar{t}}$  [5]. We can calculate the differential cross section in this variable from the results in PIM kinematics by using that, up to power corrections which vanish in the soft limit,

$$\Delta y = \ln \left( \frac{1 + \cos \theta \sqrt{1 - 4m_t^2/M_{t\bar{t}}^2}}{1 - \cos \theta \sqrt{1 - 4m_t^2/M_{t\bar{t}}^2}} \right). \quad (13)$$



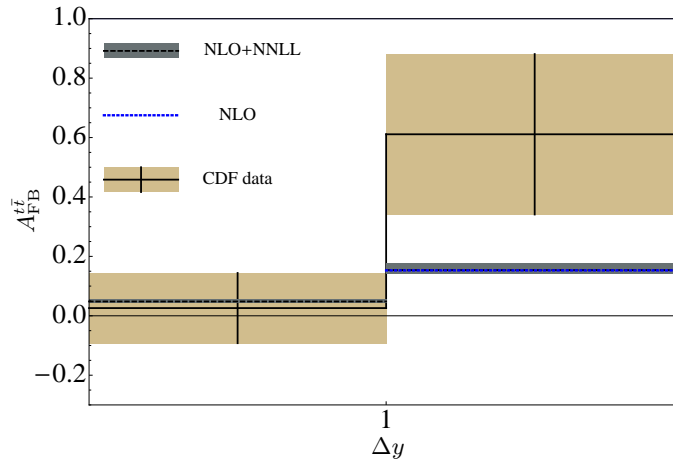


FIG. 5: The asymmetry for  $\Delta y < 1$  and  $\Delta y \geq 1$  as measured in [5], compared to our predictions at NLO+NNLL order. The bands in the NLO+NNLL results are related to uncertainties from scale variation, while the NLO result in the higher bin is evaluated at  $\mu_f = m_t$ .

	$\Delta y < 1$		$\Delta y \geq 1$	
	$\Delta\sigma_{\text{FB}}^{t\bar{t}}$ [pb]	$A_{\text{FB}}^{t\bar{t}}$ [%]	$\Delta\sigma_{\text{FB}}^{t\bar{t}}$ [pb]	$A_{\text{FB}}^{t\bar{t}}$ [%]
CDF		$2.6^{+11.8}_{-11.8}$		$61.1^{+25.6}_{-25.6}$
NLO	$0.204^{+0.105}_{-0.064}$	$4.86^{+0.42}_{-0.35}$	$0.172^{+0.094}_{-0.057}$	$15.29^{+1.26}_{-1.11}$
NLO+NNLL	$0.230^{+0.040}_{-0.035}$	$4.77^{+0.39}_{-0.35}$	$0.196^{+0.035}_{-0.031}$	$14.59^{+2.16}_{-1.30}$

TABLE IV: Comparison of  $A_{\text{FB}}^{t\bar{t}}$  for  $\Delta y < 1$  and  $\Delta y \geq 1$  with CDF data [5], along with the asymmetric cross section. The errors in the QCD predictions refer to the uncertainties related to scale variation.

After changing variables from the scattering angle to the pair rapidity difference, we express the asymmetric cross section as

$$\begin{aligned}
\Delta\sigma_{\text{FB}}^{t\bar{t}} &= \int_0^{\Delta y_+} d\Delta y \left[ \int_{M_{t\bar{t}}^{\min}}^{\sqrt{s}} dM_{t\bar{t}} \frac{d^2\sigma^{p\bar{p} \rightarrow t\bar{t}X}}{dM_{t\bar{t}}d\Delta y} - \int_{M_{t\bar{t}}^{\min}}^{\sqrt{s}} dM_{t\bar{t}} \frac{d^2\sigma^{p\bar{p} \rightarrow t\bar{t}X}}{dM_{t\bar{t}}d\Delta\bar{y}} \Big|_{\Delta\bar{y}=-\Delta y} \right] \\
&\equiv \int_0^{\Delta y_+} d\Delta y \left[ \left( \frac{d\sigma}{d\Delta y} \right)_F - \left( \frac{d\sigma}{d\Delta y} \right)_B \right] \equiv \int_0^{\Delta y_+} d\Delta y \frac{d\Delta\sigma_{\text{FB}}^{t\bar{t}}}{d\Delta y}, \quad (14)
\end{aligned}$$

where

$$\Delta y_+ = \ln \left( \frac{1 + \sqrt{1 - 4m_t^2/s}}{1 - \sqrt{1 - 4m_t^2/s}} \right) \quad \text{and} \quad M_{t\bar{t}}^{\min} = 2m_t \cosh(\Delta y/2). \quad (15)$$

Using these definitions, we can also introduce the  $\Delta y$ -dependent asymmetry

$$A_{\text{FB}}^{t\bar{t}}(\Delta y) = \frac{\frac{d\Delta\sigma_{\text{FB}}^{t\bar{t}}}{d\Delta y}}{\left( \frac{d\sigma}{d\Delta y} \right)_F + \left( \frac{d\sigma}{d\Delta y} \right)_B}, \quad (16)$$

and binned asymmetries analogous to (12), where the numerator and denominator of the above expression are integrated over a range in  $\Delta y$ . Note that the integration region above implies that higher values of  $\Delta y$  correspond to higher values of  $M_{t\bar{t}}$ . For example, the restriction  $\Delta y > 1$  used in the binned analysis below corresponds to events with  $M_{t\bar{t}} > 390$  GeV.

We show results related to the rapidity dependence of the FB asymmetry in Figures 4 and 5, and in Table IV. In all cases we use MSTW2008 PDFs. The more detailed results in the Figure 4 show the differential asymmetric cross

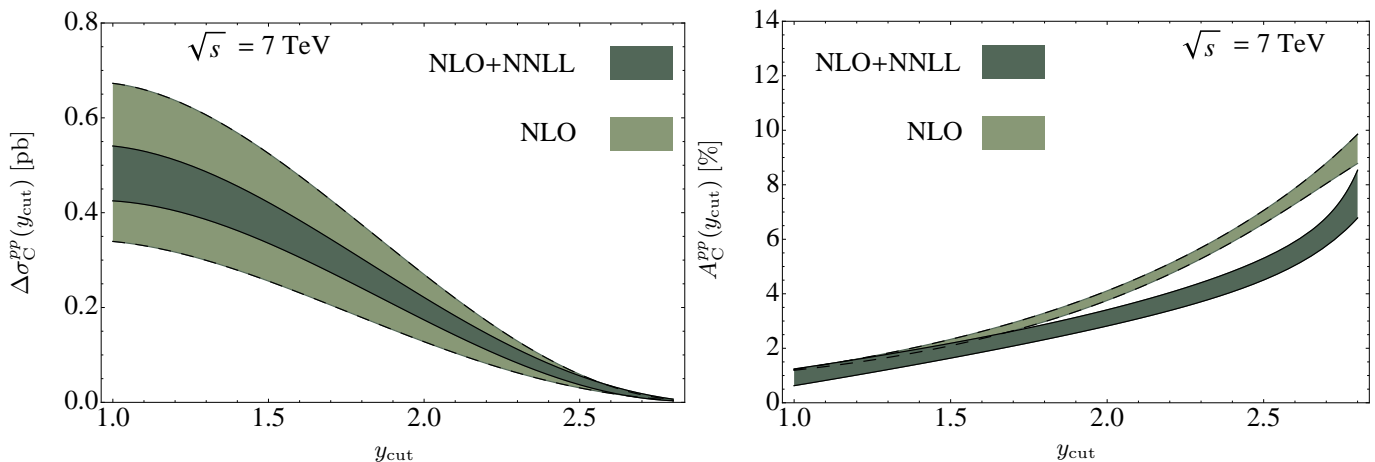


FIG. 6: Left: The partially integrated charge-asymmetric cross section  $\Delta\sigma_C^{pp}(y_{\text{cut}})$ . Right: The partially integrated charge asymmetry  $A_C^{pp}(y_{\text{cut}})$ . The bands show the uncertainties related to scale variation.

section along with the pair-rapidity dependent FB asymmetry, in the form of bands related to uncertainties from scale variations. While resummation stabilizes the asymmetric cross section compared to NLO, there is little effect on the FB asymmetry. The results for the binned asymmetry are given in Table IV, along with their visual representation in Figure 5, which shows the NLO+NNLL result with an error band from scale variations along with the default NLO number in the higher bin. For events where  $\Delta y \leq 1$ , the QCD prediction is in agreement with the CDF measurement [5]. In the bin where  $\Delta y \geq 1$ , the predicted asymmetry is lower than the measured one by  $\sim 1.5\sigma$ . Again in this case, soft-gluon resummation changes the NLO predictions only slightly.

#### IV. CHARGE ASYMMETRY AT THE LHC

The Tevatron results for the FB asymmetry at high pair invariant mass and rapidity hint at a discrepancy with the Standard Model. It would of course be desirable to study the physics responsible for this effect through measurements at the LHC.

The total and differential FB asymmetries at the LHC vanish, because of the symmetric initial state. However, while charge conjugation invariance of the strong interaction implies that the rate for the forward production of top-quarks is equal to the rate for backward production of antitop quarks at the Tevatron, this is not the case at the LHC. At a proton-proton collider the total rate for top and antitop production in the forward or backward hemisphere is equal, but at a given rapidity the rates differ. In fact, at large (small) rapidities the rate for top-quark production is noticeably larger (smaller) than that for antitop production [2], so although there is no FB asymmetry at the LHC there is a differential charge asymmetry. Like the FB asymmetry at the Tevatron, this charge asymmetry at the LHC is related to the asymmetric part of the  $q\bar{q}$  partonic cross section, implying a direct correlation between potential new physics contributions to the two measurements. The charge asymmetry at the LHC is generally smaller than the FB asymmetry at the Tevatron due to large contributions from the  $gg$  channel to the charge-symmetric part of the differential cross section, but the rapidity reach at the LHC is larger and the charge asymmetry thus provides complementary information.

In this section we study the simplest realization of a charge asymmetry at the LHC, namely the rapidity-dependent quantity in the laboratory ( $pp$ ) frame. In particular, we focus on the partially integrated charge asymmetry and charge-asymmetric cross section, where we impose the restriction  $y > y_{\text{cut}}$  on the differential cross section. We define these through

$$A_C^{pp}(y_{\text{cut}}) = \frac{\int_{y_{\text{cut}}}^{y_t^+} dy_t \left( \frac{d\sigma^{pp \rightarrow tX_{\bar{t}}}}{dy_t} - \frac{d\sigma^{pp \rightarrow \bar{t}X_t}}{dy_{\bar{t}}} \Big|_{y_{\bar{t}}=y_t} \right)}{\int_{y_{\text{cut}}}^{y_t^+} dy_t \left( \frac{d\sigma^{pp \rightarrow tX_{\bar{t}}}}{dy_t} + \frac{d\sigma^{pp \rightarrow \bar{t}X_t}}{dy_{\bar{t}}} \Big|_{y_{\bar{t}}=y_t} \right)} \equiv \frac{\Delta\sigma_C^{pp}(y_{\text{cut}})}{\int_{y_{\text{cut}}}^{y_t^+} dy_t \left( \frac{d\sigma^{pp \rightarrow tX_{\bar{t}}}}{dy_t} + \frac{d\sigma^{pp \rightarrow \bar{t}X_t}}{dy_{\bar{t}}} \Big|_{y_{\bar{t}}=y_t} \right)}, \quad (17)$$

with  $y_t^+$  as in (6).

We can study the partially integrated charge asymmetry and asymmetric cross section (17) at NLO and NLO+NNLL order using the results for the differential cross section in 1PI kinematics obtained in [7]. The results generated with MSTW2008 PDFs are shown in Figure 6, where the bands reflect uncertainties related to scale variations carried out with the same procedure as at the Tevatron. For the charge-asymmetric cross section shown in the left-hand panel of the figure, the main effect of the resummation is to decrease the scale dependence of the result to a relatively small region of the NLO error band. For the partially integrated asymmetry shown in the right-hand panel of the figure, the resummation is a mild effect up to  $y_{\text{cut}} \sim 1.5$ , but substantially reduces the asymmetry at higher values of the cut. However, due to large K factors in the gluon channel at the LHC, the uncertainty band for the NLO curve is very sensitive to whether one consistently expands the asymmetry ratio in (17). If we had deviated from our normal procedure and had not expanded the ratio, instead evaluating the denominator at NLO order, the NLO band would actually overlap quite well with the NLO+NNLL results shown in figure. The NLO+NNLL result is largely insensitive to this change of systematics—the result where both the numerator and denominator are evaluated at NLO+NNLL order is within the error band shown in the figure.

The partially integrated charge asymmetry vanishes for  $y_{\text{cut}} = 0$ , and becomes progressively larger at higher values of the cut. However, the charge asymmetric cross section shown in the left-hand side of the figure is very small at higher rapidity values and the experimental measurement is difficult. A reasonable way to compare theory and experiment in this case would be to perform a measurement in a high-rapidity bin with  $y > y_{\text{cut}} \sim 1-1.5$ . In such a bin the Standard Model charge asymmetry is predicted to be only slightly different from zero, less than 2% depending on the exact choice of the cut, so any appreciable charge asymmetry in an experimental measurement would be a clear sign of a new physics contribution to the high-rapidity region of the distribution, which is already hinted at by the Tevatron measurements.

Note that other partially integrated differential distributions can be used to study the phase-space dependence of the charge asymmetry. For instance, one can consider the so-called central charge asymmetry introduced in [29], which imposes a cut  $|y| < y_C$  along with a restriction to relatively high pair invariant mass in order to reduce the contribution from the  $gg$  channel to the symmetric part of the partially integrated cross section. Unfortunately, it is beyond the scope of the paper to perform an NLO+NNLL analysis for such an observable, because it requires a combination of PIM and 1PI kinematics which is not possible to derive starting directly from the results of [6, 7].

## V. CONCLUSIONS

The total top-quark FB asymmetry measured at the Tevatron is not in good agreement with the predictions obtained at the first non-vanishing order in perturbative QCD. The tension between theory and experiment is about two standard deviations for the asymmetry measurement in the laboratory frame, and approximately  $1\sigma$  in the top-pair rest frame. Moreover, the measurement of the asymmetry in the large pair invariant-mass region ( $M_{t\bar{t}} \geq 450$  GeV) by the CDF collaboration [5] differs from the leading-order prediction in QCD by more than three standard deviations, and there is also a discrepancy between theory and experiment for the FB asymmetry at values of the top-pair rapidity difference  $\Delta y > 1$ .

The calculations of the double differential distribution for the top-quark pair production in two different kinematic schemes, carried out in [6, 7], allow us to evaluate the FB asymmetry in both the laboratory frame and in the top-pair rest frame. The predictions obtained in this way include the full NLO corrections to the total and asymmetric cross sections, whose ratio determines the FB asymmetry, as well as the resummation of soft-gluon emission effects up to NNLL accuracy. Such NLO+NNLL results represent the most accurate determination of the QCD contribution to the asymmetry that can be obtained to date. Studies of the NLO results indicated that power corrections to our results obtained in the soft limit within the effective theory approach are small, due to the mechanism of dynamical threshold enhancement. The full NNLO calculation would be very useful in quantifying this at the next order in perturbation theory, but we do not expect such power corrections to change our predictions in any significant way.

Tables I and II show that the numerical impact of the NNLL corrections on the total asymmetry is modest, less than 3% of the central value in all cases considered. It must be observed that while the total and asymmetric cross sections calculated at NLO+NNLL order have smaller scale uncertainties than the corresponding quantities calculated at NLO, the same is not always true for the FB asymmetry, indicating that the errors at NLO are affected by accidental cancellations and do not reflect the true perturbative uncertainties. After the inclusion of the NNLL corrections, the predicted values of the asymmetry remain lower than the measured ones by  $\sim 2\sigma$  in the  $p\bar{p}$  frame and  $\sim 1\sigma$  in the  $t\bar{t}$  frame. We have also shown that PDF uncertainties are much reduced for the FB asymmetries compared to those for the asymmetric or total cross sections. For instance, the total asymmetry calculated with MSTW2008 PDFs differs from the one obtained from CTEQ6.6 or NNPDF2.1 PDFs by only a few percent.

The NLO+NNLL calculation of the asymmetry in the high invariant-mass bin  $M_{t\bar{t}} \geq 450$  GeV increases the NLO

prediction only by a very small amount, about 3% of the central value. The perturbative and PDF uncertainties of the calculation are much smaller than the experimental errors. Hence, if the Tevatron measurement of the FB asymmetry in the high invariant-mass bin is confirmed as the experimental error is reduced, it will become a compelling signal for physics beyond the Standard Model.

Given the situation at the Tevatron, it is well motivated to measure observables sensitive to the top quark asymmetry also at the LHC. Since the FB asymmetry vanishes at the LHC, one of the possible choices consists in measuring the charge asymmetry partially integrated in a given rapidity region. Starting from the NLO+NNLL resummed rapidity distributions for the top and antitop quarks, we calculated the charge asymmetry as a function of a lower rapidity cut in the laboratory frame. A careful choice of the lower bound on the rapidity integration region can allow one to use this observable to test for the presence of new physics in the top-quark sector at the LHC, thus providing complementary information to the Tevatron measurements.

*Acknowledgments:* We would like to thank Rikkert Frederix for providing us a private version of MadFKS. This research was supported in part by the State of Rhineland-Palatinate via the Research Center *Elementary Forces and Mathematical Foundations*, by the German Federal Ministry for Education and Research under grant 05H09UME, by the German Research Foundation under grant NE398/3-1, by the European Commission through the *LHCPhenoNet* Initial Training Network PITN-GA-2010-264564, and by the Schweizer Nationalfonds under grant 200020-124773.

- 
- [1] J. H. Kühn, G. Rodrigo, Phys. Rev. Lett. **81**, 49-52 (1998). [hep-ph/9802268].
  - [2] J. H. Kühn, G. Rodrigo, Phys. Rev. **D59**, 054017 (1999). [hep-ph/9807420].
  - [3] V. M. Abazov *et al.* [ D0 Collaboration ], Phys. Rev. Lett. **100**, 142002 (2008). [arXiv:0712.0851 [hep-ex]].
  - [4] T. Aaltonen *et al.* [ CDF Collaboration ], Phys. Rev. Lett. **101**, 202001 (2008). [arXiv:0806.2472 [hep-ex]].
  - [5] T. Aaltonen *et al.* [ CDF Collaboration ], Phys. Rev. **D83**, 112003 (2011). [arXiv:1101.0034 [hep-ex]].
  - [6] V. Ahrens, A. Ferroglia, M. Neubert, B. D. Pecjak, L. L. Yang, JHEP **1009**, 097 (2010). [arXiv:1003.5827 [hep-ph]].
  - [7] V. Ahrens, A. Ferroglia, M. Neubert, B. D. Pecjak, L. L. Yang, [arXiv:1103.0550 [hep-ph]].
  - [8] A. D. Martin, W. J. Stirling, R. S. Thorne, G. Watt, Eur. Phys. J. **C63**, 189-285 (2009). [arXiv:0901.0002 [hep-ph]].
  - [9] W. Bernreuther, Z. -G. Si, Nucl. Phys. **B837**, 90-121 (2010). [arXiv:1003.3926 [hep-ph]].
  - [10] J. M. Campbell and R. K. Ellis, Phys. Rev. D **60** 113006 (1999) [arXiv:hep-ph/9905386].
  - [11] K. Cheung, T. -C. Yuan, Phys. Rev. **D83**, 074006 (2011). [arXiv:1101.1445 [hep-ph]].
  - [12] Y. Bai, J. L. Hewett, J. Kaplan, T. G. Rizzo, JHEP **1103**, 003 (2011). [arXiv:1101.5203 [hep-ph]].
  - [13] E. L. Berger, Q. -H. Cao, C. -R. Chen, C. S. Li, H. Zhang, Phys. Rev. Lett. **106**, 201801 (2011). [arXiv:1101.5625 [hep-ph]].
  - [14] B. Bhattacharjee, S. S. Biswal, D. Ghosh, Phys. Rev. **D83**, 091501 (2011). [arXiv:1102.0545 [hep-ph]].
  - [15] V. Barger, W. -Y. Keung, C. -T. Yu, Phys. Lett. **B698**, 243-250 (2011). [arXiv:1102.0279 [hep-ph]].
  - [16] K. M. Patel, P. Sharma, JHEP **1104**, 085 (2011). [arXiv:1102.4736 [hep-ph]].
  - [17] Z. Ligeti, M. Schmaltz, G. M. Tavares, JHEP **1106**, 109 (2011). [arXiv:1103.2757 [hep-ph]].
  - [18] B. Grinstein, A. L. Kagan, M. Trott, J. Zupan, [arXiv:1102.3374 [hep-ph]].
  - [19] M. I. Gresham, I. -W. Kim, K. M. Zurek, [arXiv:1103.3501 [hep-ph]].
  - [20] S. Jung, A. Pierce, J. D. Wells, [arXiv:1103.4835 [hep-ph]].
  - [21] J. Shu, K. Wang, G. Zhu, [arXiv:1104.0083 [hep-ph]].
  - [22] P. M. Nadolsky, H. -L. Lai, Q. -H. Cao, J. Huston, J. Pumplin, D. Stump, W. -K. Tung, C. -P. Yuan, Phys. Rev. **D78**, 013004 (2008). [arXiv:0802.0007 [hep-ph]].
  - [23] R. D. Ball, V. Bertone, F. Cerutti, L. Del Debbio, S. Forte, A. Guffanti, J. I. Latorre, J. Rojo *et al.*, Nucl. Phys. **B849**, 296-363 (2011). [arXiv:1101.1300 [hep-ph]].
  - [24] R. Frederix, S. Frixione, F. Maltoni, T. Stelzer, JHEP **0910**, 003 (2009). [arXiv:0908.4272 [hep-ph]].
  - [25] L. G. Almeida, G. F. Sterman, W. Vogelsang, Phys. Rev. **D78**, 014008 (2008). [arXiv:0805.1885 [hep-ph]].
  - [26] T. Becher, M. Neubert, G. Xu, JHEP **0807**, 030 (2008). [arXiv:0710.0680 [hep-ph]].
  - [27] W. Bernreuther, M. Fuecker, Z. -G. Si, Phys. Rev. **D74**, 113005 (2006). [hep-ph/0610334].
  - [28] J. H. Kuhn, A. Scharf, P. Uwer, Eur. Phys. J. **C51**, 37-53 (2007). [hep-ph/0610335].
  - [29] O. Antunano, J. H. Kuhn, G. Rodrigo, Phys. Rev. **D77**, 014003 (2008). [arXiv:0709.1652 [hep-ph]].